Energy straggling of α particles in solid materials*

G. E. Hoffman and D. Powers
Baylor University, Waco, Texas 76703
(Received 12 January 1976)

The energy straggling Ω^2 of 0.5-, 1.0-, 1.5-, and 2.0-MeV α particles in thin vapor-deposited films of Ti, Cr, Co, Cu, and Ag onto a thick substrate has been measured to $\pm 6\%$ by an elastic scattering technique using a magnetic spectrometer. The measurements reveal a linear Ω^2 versus target thickness dependence and a mild increase with energy for a fixed target thickness. When Ω^2 is plotted as a function of Z_2, a decrease in energy straggling with increasing atomic number is observed, although it is considerably higher than predicted by the Bonderup-Hvelplund modification of the Lindhard statistical approach.

I. INTRODUCTION

In the past few years considerable work, both experimental[1-6] and theoretical,[7-9] has been carried out on the interaction of charged particles with matter. Theoretical calculations, based on the Lindhard formalism[10-14] of a degenerate electron gas, where electron densities are calculated from Hartree-Fock-Slater atomic wave functions,[15] clearly reveal the existence of a structure in the atomic stopping cross section dE/Ndx and in the mean excitation energy I when these quantities are plotted as a function of atomic number Z_2 of the target atom for fixed ion energy. The Lindhard formalism is found to be quite effective in predicting qualitative, but not quantitative, trends in dE/Ndx and I as a function of Z_2, for example, in the positions and amplitudes of oscillations. This success is quite interesting, especially since Fano[16] has pointed out a basic problem with the theory, namely, that the theory assumes that the average electron density is nearly constant over a wavelength of the plasma oscillations, a condition which does not hold in the interior of atoms. One way of testing the theory further is to measure and compare with another quantity, such as energy straggling, which is calculable from the same theoretical formalism.

Energy straggling was first calculated in the Lindhard formalism by Bonderup and Hvelplund[17] and later by Chu and Mayer.[18] Although energy straggling measurements exist,[17,19-24] which cover all or a portion of the velocity region of interest to the Lindhard formalism (0.1–0.5-MeV protons, 0.4–2.0-MeV α particles, etc.), none of these measurements specifically were made to study energy straggling as a function of Z_2 over a limited or extended portion of the periodic table.

The purpose of this paper is to do this for 0.5–2.0-MeV α particles in Ti, Cr, Co, and Cu ($Z_2 = 22$, 24, 27, and 29) covering the first transition series and in one element (Ag, $Z_2 = 47$) of the second transition series to subject the Lindhard formalism to further test. The work of this paper will also provide energy straggling information which is of current interest in backscattering spectrometry in the solid-state industry.[25]

II. THEORY

Bonderup and Hvelplund[17] (BH) have numerically calculated the energy straggling Ω^2_{BH} from asymptotic forms of the longitudinal dielectric constant $\epsilon^l(\vec{k}, \omega)$ of Lindhard's statistical model[11,13] as follows:

$$\frac{\Omega^2_{BH}}{\Omega^2_B} = \frac{1}{Z_2}\int_0^\infty 4\pi r^2 \rho(r)\,\frac{\Omega^2(r,v)}{\Omega^2_B}\,dr\ , \tag{1}$$

where

$$\frac{\Omega^2(r,v)}{\Omega^2_B} = 1+\left(\frac{1}{5}+\frac{\chi(r)}{\sqrt{3}}\right)\left(\frac{v_F(r)}{v}\right)^2 \ln\left(\frac{v}{v_F(r)}\right)^2 \tag{2}$$

$$= \frac{1}{(1+13\chi^2)^{1/2}}\left(\frac{v}{v_F(r)}\right)^2 . \tag{3}$$

For $v \le v_F(r)$, use (2), and for $v \ge v_F(r)$, use whichever expression gives the lower value. $v_F(r) = (\hbar/m)[3\pi\rho(r)]^{1/3}$ is the Fermi velocity, $\chi^2(r) = e^2/\pi\hbar v_F(r)$, and the Bohr value[26] for energy straggling is

$$\Omega^2_B = 4\pi Z_1^2 Z_2 e^4 N \Delta R\ . \tag{4}$$

Z_1 and Z_2 are the atomic number of the incident and target atoms, respectively, N is the number of target atoms per unit volume, ΔR is the absorber thickness, and e and m are the charge and mass of the electron. $\rho(r)$, the electron charge density, is calculated by BH from a first-order Lenz-Jensen model[27] and by Chu and Mayer[18] from the Hartree-Fock-Slater (HFS) atomic wave functions of Herman and Skillman.[15] BH point out that Eqs. (1)–(3) should give good results only when there are small contributions from the inner electrons, i.e., those that contribute according to Eq. (3). This fractional contribution is calculated

from the wave functions of Ref. 15 to be 0.30, 0.38, 0.48, 0.49, and 0.52 for 2-MeV α particles in Ti, Cr, Co, Cu, and Ag and is > 0.50 for all five elements at 0.5 MeV. Thus the BH asymptotic forms with HFS wave functions may have questionable validity for α particles below 2 MeV, but nevertheless it seems worthwhile to see if the model predicts qualitative trends in the straggling parameter Ω^2.

Williams,[28] Livingston and Bethe,[29] and Titeica[30] have derived quantum-mechanical expressions for energy straggling which are essentially within $\sim 20\%$ of the Bohr value for 1.0–2.0-MeV α particles in Ti, Cr, Co, Cu, and Ag. Bichsel[31,32] gives the relative contribution to energy straggling from K- and L-shell electrons in terms of the second moment M_2 of the collision cross section $w(\epsilon)$ for single collisions, and estimates[33] that the energy straggling should be lower than the Bohr value Ω_B^2 for these five elements in this energy region.

III. EXPERIMENTAL

The He^+ beam from a 2-MeV Van de Graaff accelerator was focused with a quadrupole magnet, analyzed with a 15° deflection magnet, trimmed to a spot size 0.159 cm wide by 0.079 cm high, and directed into a 15.24-cm-diameter scattering chamber with typical beam current 200 nA. The elastically scattered He ions were detected at laboratory scattering angle $\theta_L = 128.3°$ by a double-focusing magnetic spectrometer of 38.1 cm radius and 60° deflection angle; the spectrometer entrance aperture at a distance 5.08 cm from the scattering-chamber axis was 0.238 cm high $\times$ 0.278 cm wide, and the spectrometer exit aperture at the focal plane was $\Delta r \simeq 0.025$–0.038 cm and $\Delta z \simeq 1.016$–1.524 cm. This spectrometer provided an energy resolution typically better than 10 keV. The spectrometer energy was calibrated from the primary-beam energy and from the spectrometer magnetic field, which was obtained by conventional NMR methods. The He^+ beam, after passing through the target material, would pick up and lose electrons. The scattered beam would therefore enter the magnetic spectrometer as He^0, He^+, or He^{++}. At 1.5 and 2.0 MeV, the scattered He^{++} beam was used, at 1.0 MeV He^{++} and He^+ were used for thin and thick targets, respectively, and at 0.5 MeV the He^+ scattered beam was used exclusively.

Target elements of Ti, Cr, Co, Cu, and Ag of purity $\geq 99.5\%$ were obtained from A. D. Mackay, Inc., New York, N. Y. Thin uniform layers of these materials were vapor deposited onto Ta, Au, or Al backing materials using an electron-beam gun for all materials except Ag, where resistance heating of a Ta boat was used. A stainless-steel mask provided a circular opening of diameter 2.0088 ± 0.0069 cm on the substrate onto which the metals were evaporated. The target thickness $\rho\Delta S$ (ρ is the density, ΔS the thickness) in $\mu g/cm^2$ was obtained by differential weight measurement with a Mettler M-5 microbalance (± 2 μg error in weight) before and after deposition. The Ta backing was a thin sheet 0.010 cm thick $\times 2.54 \times 5.08$ cm of metallurgical-grade bright Sendzimer finish obtained from Fansteel Metals, North Chicago, Ill. The Al backings from United Mineral and Chemical Corp., New York, N. Y. were high-purity (99.8%) 0.159-cm-thick $\times 2.54 \times 2.54$-cm plates polished by metallurgical techniques recommended by Buehler, Ltd., Evanston, Ill. The "gold" backings were $0.159 \times 2.54 \times 5.08$-cm polished Al plates onto which high-purity gold (99.99%) from A. D. Mackay, Inc., was evaporated. The target samples were mounted on a vertical rod in the scattering chamber, and scattering spectra were obtained from the backing substrate and then from the substrate after first penetrating the evaporated layer on the substrate.

A typical elastic-scattering spectrum $Ta(\alpha, \alpha)$ is shown on the right-hand side of Fig. 1, where a beam of He^+ ions of energy $E_{10} = 1501.3$ keV is incident at angle $\theta_1 = 25.0°$ upon the Ta. The midpoint of the leading edge of the step corresponds to energy $E_{2B} = \alpha_{Ta} E_{10} = 1397.1$ keV owing to scattering at $\theta_L = 128.3°$, $\theta_2 = 29.1°$ (θ_1, θ_2, and θ_L are not coplanar) from the surface atoms of Ta. The kinematic factor α is given by

$$\alpha = \left\{ \frac{M_1 \cos\theta_L}{M_1 + M_2} + \left[\left(\frac{M_1 \cos\theta_L}{M_1 + M_2} \right)^2 + \frac{M_2 - M_1}{M_2 + M_1} \right]^2 \right\}^{1/2}, \tag{5}$$

where M_1 and M_2 are the masses of the He and Ta atoms, respectively. The finite slope of the leading edge of the Ta backscattering spectrum is due to all finite sources of instrumental resolution. This resolution includes the relative smoothness of the target surface, i.e., where the edges in the falloff of the surface nonuniformity are $> 30°$ from the surface normal, since the detector is at $\theta_2 = 29.1°$.

A spectrum of the type shown on the right-hand side of Fig. 1 can be obtained by the convolution of a step function with a Gaussian function. From the slope at the midpoint energy E_{2B}, one finds that

$$E_A - E_B = \sqrt{2\pi}\ \Omega_{inst} = \Delta E_1 , \tag{6}$$

where Ω_{inst} is the standard deviation of the Gaussian distribution comprising all finite sources of instrumental resolution. The full width at half-

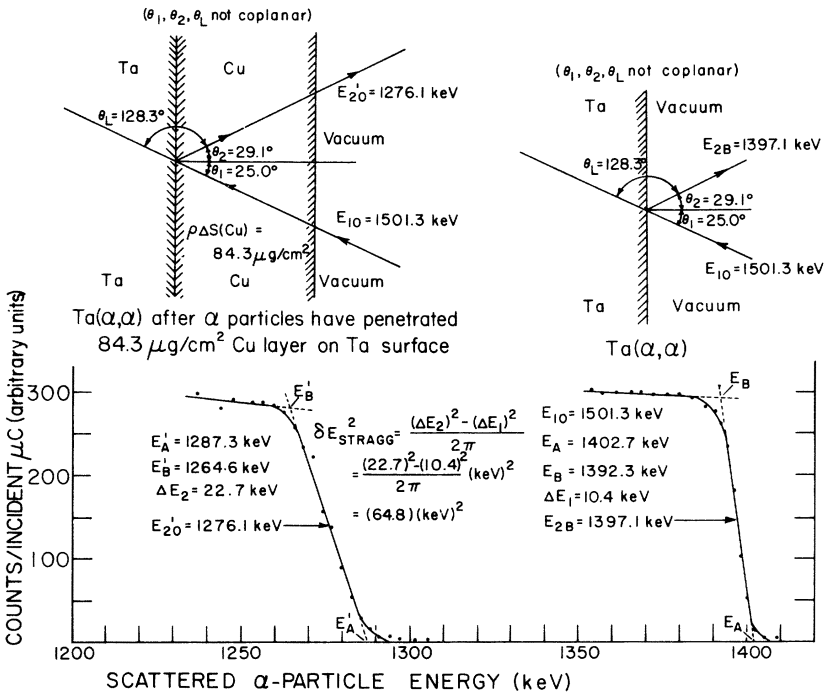

FIG. 1. Elastic scattering of α particles of incident energy $E_{10}=1501.3$ keV, first from a clean Ta backing, then from the same Ta backing onto which Cu of film thickness $\rho\Delta S=84.3$ μg/cm^2 has been evaporated. The midpoint of the leading edge of the Ta step is at $E_{2B}=\alpha_{\mathrm{Ta}}E_{10}=1397.1$ keV owing to scattering at $\theta_L=128.3°$, $\theta_2=29.1°$. The energy $\Delta E_1=E_A-E_B=10.4$ keV $=(2\pi)^{1/2}\Omega_{\mathrm{inst}}$ gives the instrumental resolution, and the energy $\Delta E_2=E'_A-E'_B=22.7$ keV $=\sqrt{2\pi}\ \Omega_2$ gives the energy spread caused by energy straggling and instrumental effects. The energy straggling is given by $\delta E^2_{\mathrm{Stragg}}\equiv\Omega^2=[(\Delta E_2)^2-(\Delta E_1)^2]/2\pi$. The energy $E'_{20}=1276.1$ keV is the energy at the magnetic spectrometer after the beam has penetrated the Cu layer, scattered from the Ta-Cu interface, and exited through the Cu layer.

maximum (FWHM) of this distribution is $(4\ln 2/\pi)^{1/2}\Delta E_1$.

The spectrum on the left-hand side of Fig. 1 corresponds to elastic scattering from the same Ta target, but after the He beam of initial energy $E_{10}=1501.3$ keV has first penetrated an evaporated Cu layer of thickness $\rho\Delta S\,(\mathrm{Cu})=84.3$ μg/cm^2 and has then exited the same layer at energy $E'_{20}=1276.1$ keV. The slope of the leading edge of Ta in this spectrum is now smaller because of energy straggling. For this spectrum, $\Delta E_2=E'_A-E'_B=22.7$ keV $=\sqrt{2\pi}\ \Omega_2$. Since the theories define energy straggling in terms of the variance Ω^2 of a Gaussian distribution, it is convenient to write

$$\delta E^2_{\mathrm{stragg}}\equiv\Omega^2=[(\Delta E_2)^2-(\Delta E_1)^2]/2\pi\ , \qquad (7)$$

where ΔE_1 and ΔE_2 are defined as E_A-E_B and $E'_A-E'_B$, respectively, as in Fig. 1.

Thus the energy straggling parameter Ω^2 is obtained by taking two spectra of the type given in Fig. 1. For both spectra, E_{10} is fixed (E_{10} is known to better than 0.1%), and the 60° spectrometer current is always monotonically decreased after careful recycling of the magnet current to eliminate hysteresis effects.

The effective thickness $\rho\Delta S$ (eff) for this reflection-type method includes both incident and exit path lengths and is given by

$$\rho\Delta S(\mathrm{eff})=\rho\Delta S\,(\alpha^2/\cos\theta_1+1/\cos\theta_2)\,, \qquad (8)$$

where α is given by Eq. (5), and $\rho\Delta S$(eff) is $2.10\rho\Delta S$, $2.111\rho\Delta S$, and $2.012\rho\Delta S$ for Ta, Au, and Al backings, respectively. For Ag on Al, the He^+ ions were scattered from the front and back surfaces of the Ag.

From the above discussion, if the energy straggling is truly Gaussian, it is essential that the rounding of the leading edge at the bottom and top of the spectrum be the same. Fano[34] has pointed out that the distributions are far from Gaussian when $T_{\max}\simeq(4m_e/M_\alpha)E_\alpha$ (m_e is the electron mass and M_α and E_α are the mass and energy of the α particle), the maximum energy imparted by the α particle to a recoil electron, is comparatively large. For a 2-MeV α particle, $T_{\max}$ is approximately equal to 1.1 keV; the thinnest target (Co) used in the experiment had an effective target thickness $\simeq 45$ μg/cm^2, and an α particle would lose[1] $\simeq 32$ keV in this target. Thus 32 keV $\gg$ 1.1 keV, and it is probably safe to assume that the straggling distributions are Gaussian. A more rigorous treatment involves the solution of the transport equation describing the energy loss of heavy charged particles in thin absorbers, for example, by Vavilov.[35] Seltzer and Berger[36] give a simple guide for testing the type of distribution

in terms of the parameter

$$\kappa = 0.300\,58 \frac{m_e c^2}{\beta^2} \frac{Z_2}{A_2} \frac{\rho S}{T_{\max}}, \tag{9}$$

where m_e is the mass of the electron, $\beta = V_\alpha/c$, Z_2 and A_2 are the atomic and mass number of the target atom, and ρS is the path length in g/cm^2. If $\kappa \gg 1$, the distribution is Gaussian; if $\kappa = 0$, the distribution is of the Landau type. For $E_\alpha = 0.5$, 1.0, 1.5, and 2.0 MeV in a 45-μg/cm^2 Co target, $\kappa = 43.0$, 10.7, 4.8, and 2.7, respectively. A plot of the Vavilov distribution $\varphi(\lambda, \kappa, \beta^2)$ vs λ for $\beta^2 = 1.07 \times 10^{-3} \simeq 0$ (2-MeV α particles) and $\kappa = 1$ shows a slight asymmetry, and for $\beta^2 \simeq 0$, $\kappa = 4$ even less asymmetry. It is therefore possible that the straggling distributions in Ti, Cr, Co, Cu, and Ag at $E_\alpha = E_{10} = 2.0$ MeV for the thinnest targets $\rho\Delta S(\text{eff}) < 100$ μg/cm^2 may have a slight asymmetry; this asymmetry was not explicit in the spectra and has not been taken into account.

Not all target thicknesses could be used because of interference effects in the scattered beam; for example, with a 36.3-μg/cm^2 Ag target on Ta at $E_{10} = 1.0$ MeV, the scattered He^+ beam from the Ag surface occurred at the same spectrometer setting as the He^{++} coming from the Ta backing after passing through the thin film of Ag. The same scattered component He^+ (or He^{++}) was always used to obtain both ΔE_1 and ΔE_2. Evaporated target uniformity was checked by obtaining spectra of the type on the left-hand side of Fig. 1 at the top, bottom, and center of the thin-film target, and using the three different E_{20}' values with the stopping powers of Ref. 1 to calculate the thickness. If the target nonuniformity exceeded 5%, the target was discarded.

Carbon buildup was minimized by cryogenic trapping to keep the vacuum $\lesssim 1 \times 10^{-6}$ Torr at all times. Any carbon buildup would cause an increase in ΔE_2 and erroneous energy straggling measurement. Any evidence of darkening of the beam target spot after the measurement indicated carbon buildup, and such data points were discarded. The beam exposure time and beam current were always approximately the same on the substrate spectrum and on the substrate-plus-thin-film spectrum.

Two or more scattering spectra of the type shown in Fig. 1 were run for each target thickness and energy. ΔE_1 was found to be quite constant for a given set of beam parameters, but ΔE_2 was found to change somewhat for the same set of beam parameters. A separate Ω^2 was obtained for each individual scattering spectrum, and the average value of Ω^2 was obtained from the separate Ω^2 values at a given energy and target thickness. These separate values differed from their average value by a fraction of a percent to occasionally as much as 20%, but were typically about 6% different. An examination of the leading edges of the separate scattering spectra (used to determine ΔE_1 and ΔE_2) by drawing different lines through the data points to determine the slope of these leading edges revealed that the change in Ω^2 was also, on the average, about 6%. It is therefore felt that a reasonable estimate of the probable error in the straggling measurement Ω^2 for a particular thickness $\rho\Delta S$ is about $\pm 6\%$.

A probable error of $\pm 5\%$ is assigned to the thicknesses $\rho\Delta S$ that are tabulated in the results. The inherent error of ± 2 μg of the deposited material makes the weight error smaller for a greater weight of deposited material. The stopping powers of Ref. 1 are typically known to $\pm 4\%$, and these are used with the energies E_{10} and E_{20}' and angles θ_1, θ_2, and θ_L of the scattering spectra to give an independent estimate of $\rho\Delta S$. These separate $\rho\Delta S$ values, on the average, are well in agreement with the weight-measured $\rho\Delta S$ values within $\pm 5\%$ for Cr and Cu at all energies, and for Co and Ag for $E_{10} \geq 1.0$ MeV. For Co and Ag at $E_{10} = 0.5$ MeV, however, the difference is 7%–8%, and at all energies in Ti the difference is from 6%–10%. The difference at 0.5 MeV may not be significant, since the stopping powers of Ref. 1 must be extrapolated outside their energy region to make the calculations of $\rho\Delta S$. The difference in Ti, however, is indicative of a lesser stopping power for Ti obtained here from that quoted in Ref. 1. Leminen and Fontell[37] have reported a similar difference in the stopping power of Ti for α particles.

IV. RESULTS

The energy-straggling parameter Ω^2 as a function of bombarding α-particle energy E_{10} was obtained from 53 different targets and from a total of 463 spectra of the type shown in Fig. 1. The number of targets and the range of thicknesses $\rho\Delta S$ for each element were as follows: Ti(10), 23.6–456.2 μg/cm^2; Cr(11), 29.9–448.1 μg/cm^2; Co(7), 21.4–202.9 μg/cm^2; Cu(14), 38.0–701.4 μg/cm^2; and Ag(11), 36.3–523.2 μg/cm^2. The number of individual spectra per element ranged from 71 in Ti to 113 in Cu. The value of Ω^2 for a small sampling[38] of the many targets is entered in Table I for $\rho\Delta S$ limited to the narrow region 29.9–38.0 μg/cm^2. This table gives a rough idea as to how the values of Ω^2 depend upon energy for a specified target thickness. The straggling values are found to be essentially independent of whether the backing material is Ta, Au, or Al.

The energy straggling values Ω^2 obtained from the spectra are plotted in Fig. 2 as a function of $\rho\Delta S(\text{eff})$ for fixed energy $E_{10} = 1.0$ MeV and are

TABLE I. Energy straggling Ω^2 as a function of bombarding energy E_{10} for a small sampling of the 53 different targets used in the experiment (but see Ref. 38). n is the number of spectra of the type in Fig. 1 used to determine Ω^2. E'_{20} is the energy at the spectrometer after scattering from the substrate-film interface. Column 3 gives the actual target thickness, column 4 the effective target thickness $=2.10\rho\Delta S$ or $2.111\rho\Delta S$ for Ta or Au backings, respectively. ΔE_1 and ΔE_2 are the instrumental and straggling-plus-instrumental spread, respectively (see Fig. 1). The last column gives the energy straggling $[(\Delta E_2)^2-(\Delta E_1)^2]/2\pi$. The backing material is Ta unless otherwise noted.

$E_{10}(n)$ (keV)	E'_{20} (keV)	$\rho\Delta S$ (μg/cm^2)	$\rho\Delta S$(eff) (μg/cm^2)	ΔE_1 (keV)	ΔE_2 (keV)	Ω^2 (keV)^2
Titanium						
1004.0(2)	859.2	32.6	68.5	9.6	17.2	32.4
1505.0(2)	1332.2	32.6	68.5	9.3	16.2	28.0
2004.1(2)	1806.4	32.6	68.5	10.1	17.0	29.7
Chromium						
503.5(3)	412.2	29.9	62.8	9.4	15.5	24.2
1005.8(4)	881.6	29.9	62.8	8.3	14.8	23.9
1502.3(4)	1347.4	29.9	62.8	8.8	15.3	24.9
2002.5(3)	1817.8	29.9	62.8	8.1	14.9	24.9
Cobalt						
1005.3(3)	878.3	33.0	69.3	9.6	15.9	25.6
1502.8(4)	1346.6	33.0	69.3	7.3	14.3	24.1
2003.5(3)	1809.9	33.0	69.3	7.6	14.5	24.3
Copper						
1003.0(2)	882.6	38.0 [a]	80.2 [a]	7.8	14.3	22.9
1504.4(3)	1352.4	38.0 [a]	80.2 [a]	7.9	14.7	24.4
2002.5(3)	1822.1	38.0 [a]	80.2 [a]	8.8	16.0	28.4
Silver						
504.9(4)	423.6	36.3	76.2	8.6	13.0	15.1
1503.3(3)	1355.6	36.3	76.2	8.4	13.4	17.3
2002.6(4)	1825.0	36.3	76.2	8.6	13.2	16.0

[a] Gold backing material.

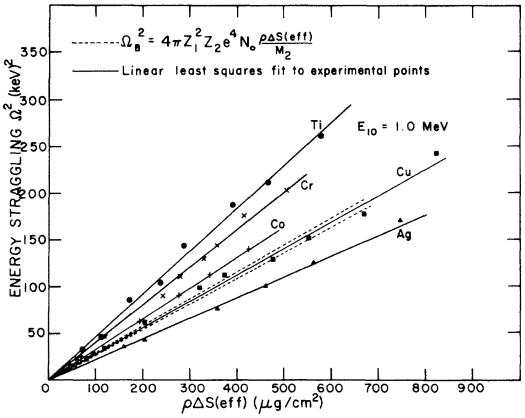

FIG. 2. Energy straggling Ω^2 as a function of target thickness $\rho\Delta S$(eff) for $E_{10}=1.0$ MeV. The experimental points are given by the different symbols. The solid lines represent the linear least-squares fit to the function $\Omega^2=a\,\rho\Delta S$(eff), where the values of a are given in Table II. The Bohr theoretical value Ω_B^2 given by Eq. (4) for the five elements Ti, Cr, Co, Cu, and Ag is restricted to the narrow band indicated by the two dotted lines.

found to be linear in form. A linear least-squares fit $\Omega^2=a\rho\Delta S$(eff) is made to the data for each element and each energy, and the values of the parameter a are entered in Table II. The five solid lines in Fig. 2 represent this least-squares fit at 1.0 MeV. This linear behavior of Ω^2 with $\rho\Delta S$(eff) is found for all five elements at all four energies $E_{10}=0.5$, 1.0, 1.5, and 2.0 MeV, and is in agreement with the linear behavior Ω_B^2 predicted by Bohr in Eq. (4). The Bohr value Ω_B^2 for the five elements, however, is restricted to the narrow band indicated by the two dotted lines in Fig. 2, and does not adequately predict the broad Z_2 variation in Ω^2 found in this experiment.

TABLE II. Slope a of least-squares fit $\Omega^2=a\rho\Delta S$(eff) to energy straggling data of Table I.

E_{10} (MeV)	Ti	Cr	Co	Cu	Ag
0.5	0.4438	0.3795	0.3267	0.2896	0.2108
1.0	0.4608	0.4042	0.3296	0.2843	0.2233
1.5	0.4715	0.4064	0.3344	0.3021	0.2326
2.0	0.4814	0.4039	0.3342	0.2914	0.2344

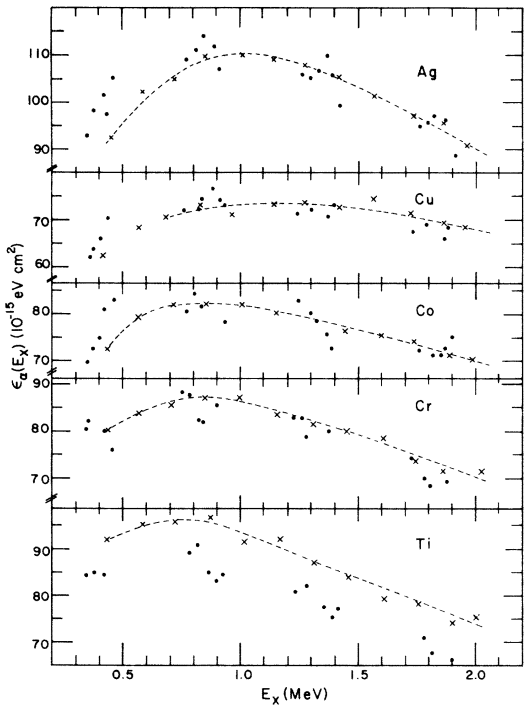

FIG. 3. Stopping cross section $\epsilon_\alpha(E_x)$ for Ti, Cr, Co, Cu, and Ag obtained from the experimental data by the method of Warters (Ref. 39), where $\epsilon_\alpha(E_x) = (\alpha_{Ta}E_{10} - E'_{20})/B$, $B = (N_0\rho\Delta S/M_2)(\alpha_{Ta}+\beta)/\cos\theta_1$, $E_x \simeq (\alpha_{Ta}E_{10} + \beta E'_{20})/(\alpha_{Ta}+\beta)$, $\beta = (\cos\theta_1)/(\cos\theta_2)$, $\alpha_{Ta} = 0.930\,83$, and N_0 is Avogadro's number. Only Ta backings are used and $\rho\Delta S \leq 276$ μg/cm^2. The $\times$'s and dashed curves are the values given by Chu and Powers (Ref. 1), and the closed circles are obtained from the present measurements.

A slight dependence of Ω^2 with E_{10} may be seen from Table II. The slope a is seen to increase in Ti, Cr, and Ag from $E_{10} = 0.5$ to 2.0 MeV by 8.1%, 6.1%, and 10.5%, respectively, but is essentially constant in Co and Cu. The Bohr prediction Ω_B^2 given by Eq. (4) is independent of energy, and the Bonderup-Hvelplund modification using HFS atomic charge densities predicts an increase in Ω_{BH}^2 with energy of 85%, 102%, 106%, 116%, and 120% for Ti, Cr, Co, Cu, and Ag, respectively, from $E_{10} = 0.5$ to 2.0 MeV. Thus the slight energy dependence of Ω^2 is more consistent with the Bohr approach than the Bonderup-Hvelplund approach. This great discrepancy in the latter approach may be due to the large contribution to Ω_{BH}^2 from the inner electrons, as is pointed out in the theory.

The stopping cross sections $\epsilon_\alpha(E_x) = dE/Ndx$ of Ti, Cr, Co, Cu, and Ag have been calculated by the method of Warters[39] for $\rho\Delta S \leq 276$ μg/cm^2 and are compared to the values of Chu and Powers[1] in Fig. 3 as an independent check on the energy straggling measurements. The ϵ_α values are in essential agreement for Cr, Co, Cu, and Ag except at $E_x \simeq 0.4$ MeV where the present measurements are $\simeq$5%–8% higher. For Ti, the ϵ_α values are lower at all energies than those of Ref. 1 by $\simeq$7%–12%. Lin and Matteson[40] suggest that the lower ϵ_α values of Chu and Powers at $E_x \simeq 0.4$ MeV may be due to their method of energy calibration for their solid-state detector. The difference in Ti, however, is more serious; Leminen[37] reports a lower ϵ_α for Ti than Chu and Powers by $\simeq$20%. It is unlikely that the $\rho\Delta S$ measurements for Ti would be off by 7%–12% in the present experiment, since the Ti measurements were made with the same apparatus after the Cu measurements and before the Cr measurements, and these latter elements did not show such an effect. If the Ti targets of the present experiment were contaminated by C from the C crucible in the electron-beam apparatus, it is estimated from a simple calculation based on the Bragg rule for stopping cross sections and on the Bohr theory for energy straggling that the energy straggling measurements of Ti would be low by no more than 2.8%. This calculation is based upon a mole fraction of 0.16 for C and 0.84 for Ti; these mole fractions would bring the solid points for Ti in Fig. 3 into agreement with the dashed curve.

In Fig. 4 the energy straggling Ω^2 is plotted as a

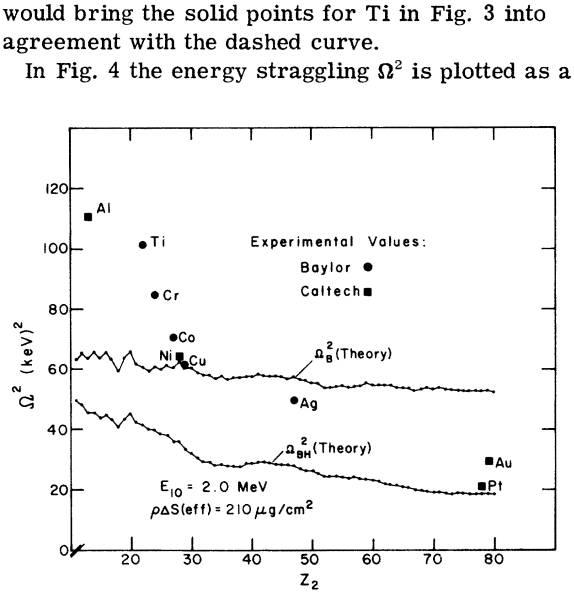

FIG. 4. Comparison of experimental and theoretical values of energy straggling as a function of atomic number Z_2 for $E_{10} = 2.0$ MeV and $\rho\Delta S$(eff) = 210 μg/cm^2. The Bohr prediction Ω_B^2 is given by Eq. (4), and the Bonderup-Hvelplund prediction with HSF atomic charge densities is given by Eqs. (1)–(3). The Al, Ni, Au, and Pt measurements by Harris *et al.*[23,24] at $E_{10} = 2.0$ MeV have been fitted by the linear function $\Omega^2 = a'\rho\Delta S$(eff) in order to make comparison to the present measurements. Neither theory quantitatively predicts the observed behavior.

function of atomic number Z_2 of the target material for $E_{10} = 2.0$ MeV and $\rho\Delta S(\text{eff}) = 210$ $\mu g/cm^2$ ($\rho\Delta S = 100$ $\mu g/cm^2$). The Al, Ni, Au, and Pt measurements by Harris *et al.*[23,24] at $E_{10} = 2.0$ MeV have also been fitted by the linear function $\Omega^2 = a' \rho\Delta S$ (eff) in order to make comparison to the present measurements; a $\rho\Delta S$(eff) value of 210 $\mu g/cm^2$ would correspond in their scattering geometry to $\rho\Delta S = 112$ $\mu g/cm^2$. The values of Ω_B^2 and Ω_{BH}^2 with HFS atomic charge densities are also plotted in Fig. 4. Similar plots of Ω^2 as a function of Z_2 at $E_{10} = 1.0$ and 1.5 MeV reveal the same behavior. Ω_{BH}^2 gives a greater decrease with Z_2 than Ω_B^2, but neither theory predicts the observed behavior quantitatively.

Bichsel[33] has pointed out that surface preparation is extremely important in an energy straggling experiment of this type, and that any surface irregularity would cause a higher straggling value. He anticipates that all the experimental values of Ω^2 should be $\leq \Omega_B^2$. Every care was made in target preparation that could be made; the three different backing materials Ta, Au, and Al made little difference in the results. The smallest polishing abrasive was 0.03 μm (the smallest available from Buehler, Ltd.), and it is clear that the samples will have at least this degree of surface irregularity. The agreement of Ω^2 for Ni and Cu found by two different groups (Caltech and Baylor) is encouraging, since both elements have approximately the same atomic number and should therefore have approximately the same energy straggling values.

In conclusion, the Lindhard formalism of a degenerate electron gas as applied to energy straggling in the Bonderup-Hvelplund modification with Hartree-Fock-Slater atomic charge densities does not quantitatively predict the observed energy dependence and Z_2 dependence of Ω^2. A mild increase (6%–10%) in Ω^2 with increasing energy (0.5–2.0 MeV) is observed, whereas an increase of ~100% is predicted; a decrease in Ω^2 with Z_2 from ~100 to ~20 is observed, whereas a decrease from ~50 to ~20 is predicted.

---

*Research supported by the Robert A. Welch Foundation, Houston, Texas 77002.

[1]W. K. Chu and D. Powers, Phys. Rev. 187, 478 (1969).
[2]W. K. Chu and D. Powers, Phys. Rev. B 4, 10 (1971).
[3]D. Powers, W. K. Chu, R. J. Robinson, and A. S. Lodhi, Phys. Rev. A 6, 1424 (1972).
[4]W. K. Lin, H. G. Olson, and D. Powers, Phys. Rev. B 8, 1881 (1973).
[5]W. K. Lin, H. G. Olson, and D. Powers, J. Appl. Phys. 44, 3631 (1973).
[6]W. K. Lin, S. Matteson, and D. Powers, Phys. Rev. B 10, 3746 (1974).
[7]C. C. Rousseau, W. K. Chu, and D. Powers, Phys. Rev. A 4, 1066 (1971).
[8]W. K. Chu and D. Powers, Phys. Lett. 38A, 267 (1972).
[9]W. K. Chu and D. Powers, Phys. Lett. 40A, 23 (1972).
[10]J. Lindhard and M. Scharff, K. Dan. Vidensk. Selsk. Mat.-Fys. Medd. 27, No. 15 (1953).
[11]J. Lindhard, K. Dan. Vidensk. Selsk. Mat.-Fys. Medd. 28, No. 8 (1954).
[12]J. Lindhard and M. Scharff, in NAS-NRC Publication No. 752, edited by Edwin A. Uehling (U.S. GPO, Washington, D. C., 1960) p. 49.
[13]J. Lindhard and A. Winther, K. Dan. Vidensk. Selsk. Mat.-Fys. Medd. 34, No. 4 (1964).
[14]E. Bonderup, K. Dan. Vidensk. Selsk. Mat.-Fys. Medd. 34, No. 17 (1967).
[15]F. Herman and S. Skillman, *Atomic Structure Calculations* (Prentice-Hall, Englewood Cliffs, N. J., 1963).
[16]U. Fano, in Ref. 12, p. 163.
[17]E. Bonderup and P. Hvelplund, Phys. Rev. A 4, 562 (1971).
[18]W. K. Chu and J. W. Mayer (unpublished).
[19]C. B. Madsen and P. Venkateswarlu, Phys. Rev. 74, 1782 (1948).
[20]C. B. Madsen, K. Dan. Vidensk. Selsk. Mat.-Fys. Medd. 27, No. 13 (1953).
[21]L. P. Nielsen, K. Dan. Vidensk. Selsk. Mat.-Fys. Medd. 33, No. 6 (1961).
[22]E. Leminen and A. Anttila, Ann. Acad. Sci. Fenn. A 6, No. 370 (1971).
[23]J. M. Harris, W. K. Chu, and M-A. Nicolet, Thin Solid Films 19, 259 (1973).
[24]J. M. Harris and M-A. Nicolet, Phys. Rev. B 11, 1013 (1975).
[25]W. K. Chu, J. W. Mayer, M-A. Nicolet, T. M. Buck, G. Amsel, and F. Eisen, Thin Solid Films 17, 1 (1973).
[26]N. Bohr, K. Dan. Vidensk. Selsk. Mat.-Fys. Medd. 18, No. 8 (1948).
[27]H. Jensen, Z. Phys. 77, 722 (1932).
[28]E. J. Williams, Proc. R. Soc. A 135, 108 (1932).
[29]M. S. Livingston and H. A. Bethe, Rev. Mod. Phys. 9, 245 (1937).
[30]S. Titeica, Bull. Soc. Roum. Phys. 38, 81 (1937).
[31]Hans Bichsel, Phys. Rev. B 1, 2854 (1970).
[32]Hans Bichsel, Phys. Rev. A 9, 571 (1974).
[33]Hans Bichsel (private communication).
[34]U. Fano, Annu. Rev. Nucl. Sci. 13, 1 (1963).
[35]P. V. Vavilov, Zh. Eksp. Teor. Fiz. 32, 320 (1957) [Sov. Phys.-JETP 5, 749 (1957)].
[36]S. M. Seltzer and M. J. Berger, in NAS-NRC publication No. 1133 (U.S. GPO, Washington, D.C., 1964), p. 187.
[37]E. Leminen and A. Fontell, Radiat. Eff. 22, 39 (1974).
[38]The complete table is on deposit with the Physics Auxiliary Publications Service (PAPS). See AIP document No. PAPS 760322-1, 6 pages. Order by PAPS number and journal reference from the American Institute of Physics, PAPS, 335 E. 45th St., N.Y., N.Y. 10017. Remit in advance $1.50 for each microfiche, or $5.00 for photocopies (airmail additional). This material also appears in *Current Physics Microfilm* on the frames immediately following this article.
[39]W. D. Warters, Ph.D. thesis (California Institute of Technology, 1953) (unpublished).
[40]W. K. Lin and S. Matteson (private communication).